Int. J. Electrochem. Sci., 15 **(2020)** 3740 – 3749, doi: 10.20964/2020.05.77

International Journal of
ELECTROCHEMICAL
SCIENCE
www.electrochemsci.org

Short Communication

Incorporation of Silicon Fume and Fly Ash as Partial Replacement of Portland Cement in Reinforced Concrete: Electrochemical study on corrosion behavior of 316LN stainless steel rebar

Caihong Zhang[1,*], *Fangfang Zhang*[2]

[1] Shaanxi Key Laboratory of Safety and Durability of Concrete Structures, Xijing University, Xian 710123, China
[2] Henan University of Science and Technology, Luoyang 471003, China
[*]E-mail: zchxjxy926@163.com

Received: 16 Janaury 2020 / *Accepted:* 3 March 2020 / *Published:* 10 April 2020

In this work, corrosion behavior of 316LN stainless steel reinforced concrete incorporated by silicon fume (SF) and fly ash (FA) as partial replacement of Portland cement were investigated. Electrochemical impedance spectroscopy (EIS), polarization resistance measurement and open-circuit potential monitoring were used to study the corrosion behavior of stainless steel rebar. The 316LN stainless steel reinforced concrete samples were exposed to 3.5 wt% NaCl solution as a marine environment. The electrochemical results showed that the steel reinforced concrete incorporated by SF and FA indicated the best corrosion behavior. The potential corrosion values were mainly related to region of 10% corrosion probability. The corrosion current density results indicated passivity state for concrete sample containing both FA and SF after 220 days of exposure time, and low corrosion probability during the experiment period. The EIS results showed that the value of double-layer capacitance decreased for the sample containing both FA and SF, indicating the passive film thickness increased and the resulting protective capacity enhanced. These results indicated that partial replacement of FA and SF simultaneously in Portland cement led to a reduced corrosion rate and enhanced corrosion resistance of steel rebar due to the reduction of water and chloride ion permeability.

Keywords: Corrosion resistance; Portland cement; Silicon fume; Fly ash; Electrochemical impedance spectroscopy; Polarization resistance

1. INTRODUCTION

The use of waste materials is one of the main approaches to reduce the environmental influence of the concrete industry [1]. The first strategy involves the replacement of cement by variable amounts

of industrial by-products [2, 3]. The use of these by-products is very common today. However, other pozzolanic materials such as metakaolin, sewage sludge ash, rice husk ash, and calcined clays have been effectively implemented in cement yields, although their use are not prolonged [4-7].

Recently, fly ash (FA) had been used in concrete as a cement replacement material for several environmental and economic reasons. There were some studies in concerning the corrosion behavior of steel rebar embedded in these cement–FA mortar and concrete mixtures [8-10]. Most researches claimed that FA additives in the presence of chloride ions had a positive effect on rebar corrosion [11]. Diaz-Loya et al. performed studies on the mechanical properties of cements containing different FA particle sizes [12]. Chahal et al. investigated the influence of fly ash on chloride permeability in concrete [13]. It was found that FA concrete increased the electrical resistance and the resistance to penetration of chloride ion [14].

Furthermore, incorporation of silica fume (SF) in concrete can increase the durability because of its ultra-fine particles [15]. The total porosity might not change with the addition of SF but the large pores can be divided into small pores and thus changing the cement paste microstructure. Bleszynski et al. revealed that addition of 8% SF can significantly reduce chloride penetration [16]. Hou and Chung investigated the effect of SF on the corrosion behavior of steel rebar in concrete by measuring the corrosion current density and corrosion potential during immersion in NaCl and $Ca(OH)_2$ solutions [17].

Given that the simultaneous effects of the FA and SF on the corrosion resistance of reinforced concrete had not been previously reported. Here, the electrochemical study on corrosion behavior of reinforced concrete incorporated with SF and FA as partial replacement of Portland cement were investigated. Electrochemical impedance spectroscopy (EIS), polarization resistance measurement and open-circuit potential (OCP) monitoring were used to study the corrosion behavior of stainless steel rebar.

2. MATERIALS AND METHOD

In this study, the mixture proportions of reinforced concrete which contained different components of cementitious materials such as Portland cement (PC), silica fume (SF) and fly ash (FA) were investigated. Properties of the mineral and cement admixtures are exhibited in Table 1.

Table 1. Chemical properties of cement, SF and FA

	PC (wt%)	SF (wt%)	FA (wt%)
SiO_2	20.65	87.74	48.05
Al_2O_3	4.74	0.00	21.56
Fe_2O_3	3.02	0.98	7.31
CaO	64.25	2.34	1.61
MgO	2.04	6.53	7.52
K_2O	0.65	3.13	3.04
Na_2O	0.27	1.58	1.58
SO_3	2.96	2.78	2.76
LOI	0.88	6.28	0.45

The proportions of mixtures for every sample are determined in Table 2. The prepared mixes were poured into the rectangular prism molds with dimensions 50×50×150 mm, and then kept at room temperature with 90% relative humidity for one day.

Table 2. The mixture proportions of reinforced concrete

Sample no.	PC (wt%)	SF (wt%)	FA (wt%)
1	100	0	0
2	75	25	0
3	75	0	25
4	50	25	25

In order to consider the effect of SF and FA incorporations on corrosion behavior of the reinforced concretes, electrochemical experiments were done on 316LN austenitic stainless steel rebar. The composition of the 316LN stainless steel rebar is indicated in Table 3.

Table 3. The composition of the 316LN stainless steel rebar (wt%)

C	Mn	Si	P	S	Nb	Cu	Mo	Nb	Cr	Ni	Fe
0.025	1.55	0.28	0.044	0.01	0.032	0.56	2.4	0.032	18.14	11.9	Residual

The three-electrode electrochemical cell was utilized to investigate the electrochemical impedance spectroscopy (EIS) of the samples. Steel reinforced concretes were applied as a working electrode and a standard copper/copper sulfate (Cu/CuSO4, CSE) electrode was used as a reference electrode. The graphite was applied as the counter electrode.

The corrosion potential (half-cell rebar/concrete) measurements was recorded for each samples according to ASTM C876-15 standards. The data was collected every three weeks for the reinforced concrete samples exposed to the 3.5 wt% NaCl electrolyte solution. The analyses of the obtained results were performed using specialized software. EIS characterizations were performed in the frequency varied between 100 kHz and 0.1 mHz at the open circuit potential (OCP) with AC perturbation ±10 mV. The polarization (CorrTest Instruments Corp., Ltd., China) measurement was conducted from 0.25V at 1 mV/s scanning rate. The morphologies of the samples were examined using scanning electron microscope (SEM, FEI/Nova NanoSEM 450).

3. RESULTS AND DISCUSSION

Concrete samples reinforced with 316LN austenitic stainless steel made with 100% PC (Sample 1), 75 wt% PC + 25 wt% SF (sample 2), 75 wt% PC + 25 wt% FA (sample 3) and 50 wt% PC + 25 wt% SF + 25 wt% FA (sample 4) indicated that, the sample 3 and 4 revealed a 10% probability of corrosion at all times exposure to NaCl solution, with corrosion potential > -200 mV. Sample 1 and 2 exhibited an uncertain corrosion from 120 to 220 days with the potential values between -200 mV and

-300 mV vs. CSE, related to the small separation of the passive layer or initiation of pitting corrosion [18].

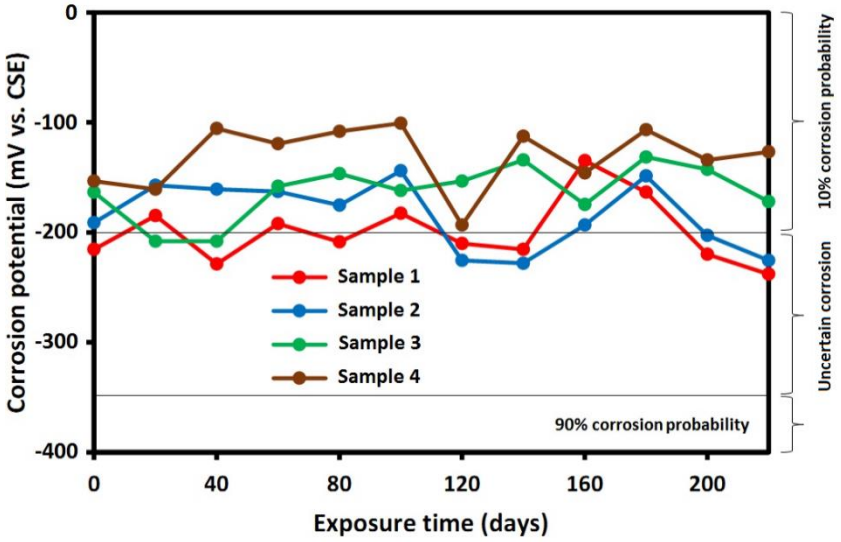

Figure 1. Corrosion potential for 316LN austenitic stainless steel embedded in different concrete samples exposed to 3.5 wt% NaCl solution

The corrosion potential values for sample 4 with 50 wt% CPC + 25 wt% SF + 25 wt% FA indicated a more stable potential value than the other samples, where their potential values remained completely in 10% corrosion probability region. One of the most important properties of the FA is its significant influence on the durability of concrete [19], which is due to the decrease in calcium hydroxide, solubility of hydration products and change in pore solution.

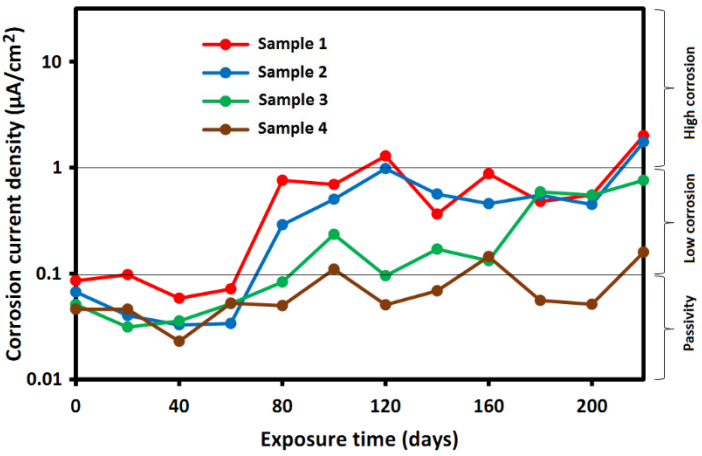

Figure 2. Corrosion current density for 316LN austenitic stainless steel embedded in different concrete samples exposed to 3.5 wt% NaCl solution

Furthermore, more corrosion resistance in the sample 4 can be associated to the SF that had reacted with the released calcium hydroxide during the cement hydration and formed additional calcium silicate hydrate, which improved the mechanical properties and durability of the concrete [20].

The corrosion current density results revealed passivity state for concrete sample containing both FA and SF after 220 days of exposure time, and low corrosion probability during the experiment period.

Figure 2 shows corrosion current density for 316LN austenitic stainless steel embedded in different concrete samples. The sample 1 with concrete containing only PC had a current density < 0.1 µA/cm^2 for first 60 days and then, it was in the low corrosion state. The passive layer formed on stainless steel rebar contained a two-layer oxide structure, the chromium and iron oxides in the inner and outer layers, respectively [21]. In the present alkaline environment, the high Ni content in the 316LN stainless steel reinforcement might play a role in corrosion resistance [22]. In the last evaluation period (200–220 days), sample 1 revealed a corrosion current density of 3 µA/cm^2, indicating the use of 316LN stainless steel rebar in high chloride environments is one of the best options for attaining more durable concrete structures which in accordance with previous studies [23-25]. Sample 2 showed similar corrosion behavior to sample 3, with lower corrosion current density during the evaluation period compared to the sample 1 manufactured without addition of admixtures. Furthermore, sample 4 exhibited better corrosion behavior than all samples, with corrosion current density of 0.1 µA/cm^2 during 140 days, indicating the passive state of reinforced concrete within the whole period. This result can be attributed to the continuous hydration of cement which had changed the structure of the concrete and led to the decrease of the chloride ions penetration in prolonged periods.

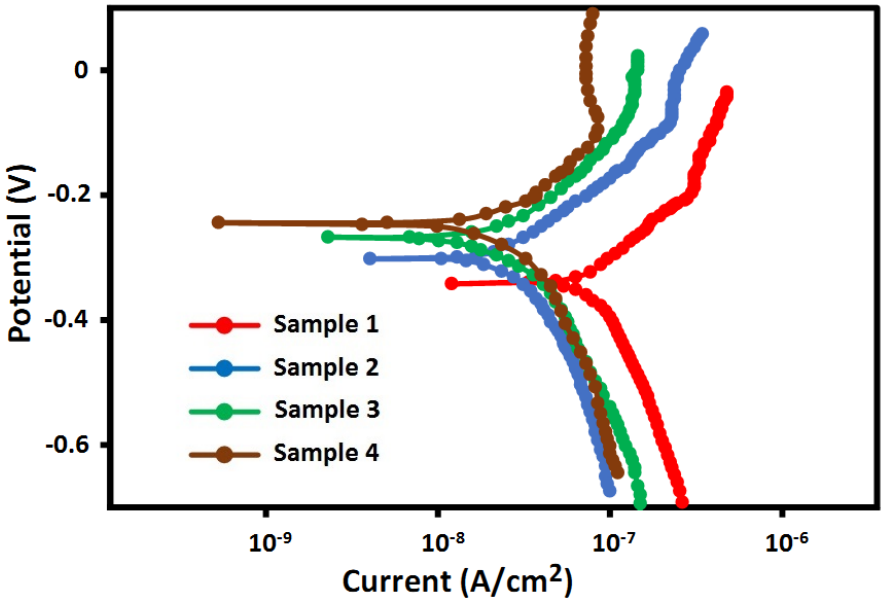

Figure 3. Potentiodynamic polarisation of 316LN austenitic stainless steel embedded in different concrete samples exposed to 3.5 wt% NaCl solution after 40 days exposure time

Figure 3 indicates polarization plots of 316LN austenitic stainless steel embedded in different concrete samples exposed to 3.5 wt% NaCl solution after 40 days exposure time in OCP conditions. As shown in figure 3, the anodic branch of polarization diagrams are considered by passive regions at all reinforcement steels, indicating that the passive films had obviously formed on the steel surface when they were exposed to the corrosive environment [26]. Furthermore, a significant shift appeared

in corrosion potential towards a positive direction which indicated that the anodic metal dissolution retarded efficiently by changing the content of concrete [27]. Compared to all the samples, the passive region is much wider at the sample 4 (50 wt% PC + 25 wt% SF + 25 wt% FA) which indicated a tendency of the steel rebar to passivate. It can be attributed to the dissolution and formation of the oxide film [28]. Moreover, the greater decrease in passive current density in sample 4 was due to a change in structure or an increase in thickness of the passive film [29].

Table 4. Corrosion potential and current density of the 316LN stainless steel rebars

Sample no.	Corrosion current density	Corrosion potential
1	0.085 μA/cm^2	-0.342 V
2	0.042 μA/cm^2	-0.315 V
3	0.027 μA/cm^2	-0.261 V
4	0.013 μA/cm^2	-0.237 V

The values of corrosion potential and corrosion current density are revealed in table 4 which is attained from the polarization curves in Figure 3.

As shown in table 5, the corrosion level can be defined into four levels proposed by Durar Network Specification [30].

Table 5. Corrosion level

Corrosion level	Corrosion current density (i_{corr}) range
Very high	1.0 μA/cm^2 < i_{corr}
High	0.5 μA/cm^2 < i_{corr} < 1.0 μA/cm^2
Low	0.1 μA/ cm^2 < i_{corr} < 0.5 μA/cm^2
Passivity	i_{corr} < 0.1 μA/cm^2

However, based on table 4, the corrosion current density of sample 4 in 3.5 wt% NaCl solution was lower than that of the other samples. Therefore, all steel reinforced concretes remained completely in the passive state during the test which indicated their good corrosion resistance in the marine environment [31].

Electrochemical technique has been widely employed in the analysis of the passive layer due to its capability to characterize redox reactions of steel rebars in a marine environment. EIS was used to analyze the corrosion behavior of 316LN austenitic stainless steel rebar in different concrete samples with passive layers in 3.5 wt% NaCl solution after 40 days exposure time. Figure 4 reveals Nyquist plots of the samples. The changes in concrete content had led to a variation in the radius of the capacitive loop which indicated an enhancement of the corrosion resistance for stainless steel rebar. Figure 5 indicates an equivalent circuit used to model the impedance spectra. R_s is the solution resistance. R_f and R_{ct} are the resistance of passive film and the charge-transfer resistance, respectively. CPE_f and CPE_{dl} are the passive film/solution interface capacitance and double-layer capacitance [32].

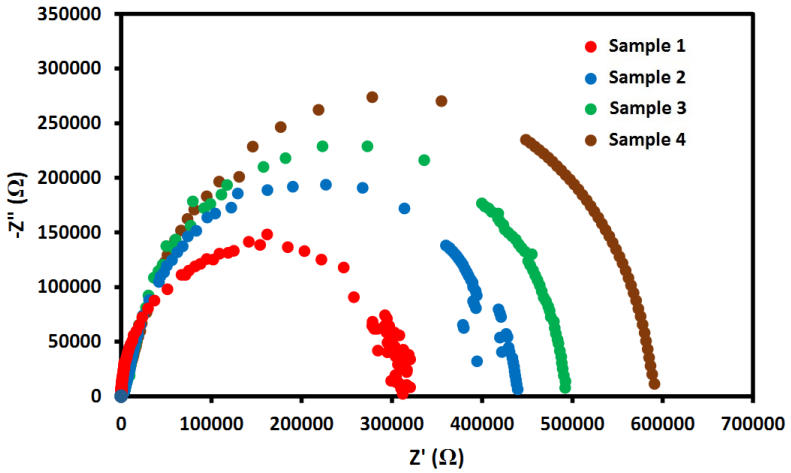

Figure 4. Nyquist diagram of 316LN austenitic stainless steel embedded in different concrete samples exposed to 3.5 wt% NaCl solution after 40 days exposure time

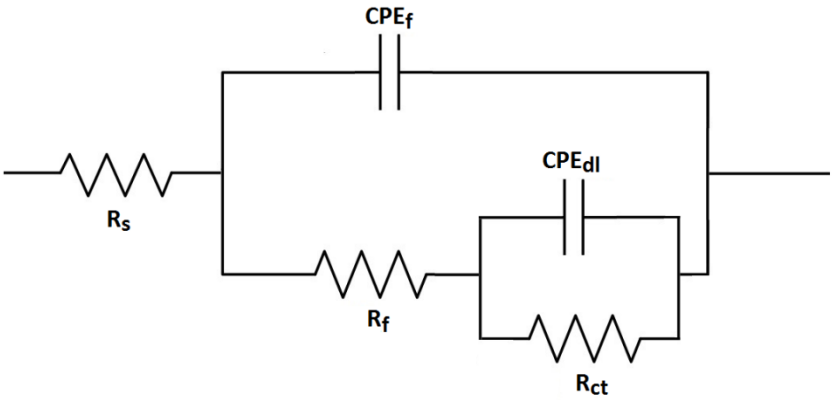

Figure 5. An equivalent circuit model to fit the experimental data

Polarization resistance, R_p (R_p = R_f + R_{ct}) is a computable indicator to consider the steel corrosion resistance in the corrosive environment [33]. So, the higher R_p value indicates higher corrosion resistance of the sample.

Table 6. Electrochemical parameters from the fitting using the equivalent circuit in Figure 5 for 316LN austenitic stainless steel embedded in different concrete samples exposed to 3.5 wt% NaCl solution after 40 days exposure time

Sample no.	R_s (Ω cm^2)	R_f (MΩ cm^2)	CPE_f (μF cm^{-2})	R_{ct} (MΩ cm^2)	CPE_{dl} (μF cm^{-2})
1	67.4	0.153	2.5	0.315	3.4
2	63.2	0.216	2.2	0.443	2.7
3	49.8	0.286	1.8	0.492	2.3
4	64.7	0.321	1.4	0.596	1.7

According to table 3, Sample 4 show a significantly enhancement in R_p value indicating a higher corrosion resistance in 3.5 wt% NaCl solution. As shown in table 6, the value of CPE_{dl}

decreased for sample 4, which reveals that the passive film thickness increased and the resulting protective capacity enhanced when the concrete content was containing both FA and SF. Furthermore, the R_f passive film resistance increased in sample 4, which indicated that the protective feature of the passive film developed was strong. The SF had a pozzolanic reaction with the $Ca(OH)_2$ crystals and produced an insoluble, dense and monolithic gel of calcium hydroxide [34, 35]. Furthermore, the FA can form a very robust adhesion to hydrated cement because of the high surface area which had led to a better inhibition of the calcium hydroxide growth. The mineral admixtures filled the capillary pores and tiny cracks and finally shrunk the cement structure [36]. These agents increased the corrosion resistance of the reinforcement steel bars in aggressive solutions. Compared to CPE_f and CPE_{dl}, it was found that CPE_f was lower than CPE_{dl} in all samples which confirmed that the formation of the thin passive film and the double layer at the interfaces had a high capacitive behavior.

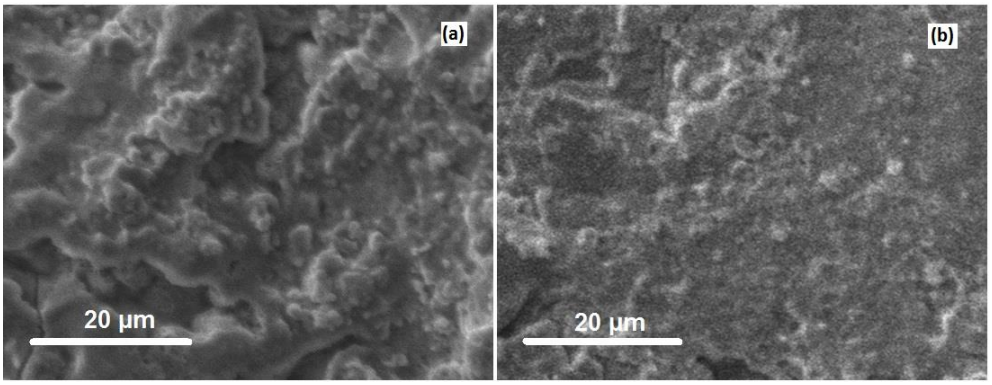

Figure 6. SEM images of stainless steel surface for (a) sample 1 and (b) sample 4 after exposed to 3.5 wt% NaCl solution for 40 days

Figure 6 indicates the SEM images of stainless steel surface of sample 1 and sample 4 after being exposed to 3.5 wt% NaCl solution for 40 days. The surface of sample 4 reveals low corrosion products and pits, indicating a mild pitting corrosion occurred on the surface of stainless steel rebar, which is consistent with the results extracted from electrochemical tests. It can be attributed to the reduction of water and chloride ion permeability in concrete sample. The SF reaction with the calcium hydroxide can produce hydration products which strongly reduce the concrete porosity. Furthermore, concrete structure can be affected by the incorporation of FA in the concrete mixture [37]. However, the total porosity cannot change with the SF addition, but the large pores can be transformed into smaller pores and thereby altering the cement paste microstructure. This result indicates that partial replacement of FA and SF simultaneously in Portland cement had led to a reduced corrosion rate and enhanced corrosion resistance of steel rebar due to the reduction of water and chloride ion permeability.

4. CONCLUSIONS

Recently, pozzolanic materials had been used in concrete as a cement replacement material for environmental and economic reasons. Here, electrochemical study on corrosion behavior of 316LN

stainless steel reinforced concrete incorporated with SF and FA as partial replacement of Portland cement were investigated. EIS, polarization resistance measurement and OCP monitoring were used to study the corrosion behavior of stainless steel rebar. The 316LN stainless steel reinforced concrete samples were exposed to 3.5 wt% NaCl solution as a marine environment. The electrochemical results showed that the steel reinforced concrete incorporated with SF and FA indicated the best corrosion behavior. The potential corrosion values were mainly related to the region of 10% corrosion probability. The EIS results showed that the value of the double-layer capacitance decreased for the sample containing both FA and SF, indicating the passive film thickness had increased and resulting in an enhanced protective capacity. These results can be attributed to the reduction of water and chloride ion permeability in the concrete sample. The FA reacted with calcium hydroxide $Ca(OH)_2$ and produced hydration products which had strongly reduced the concrete porosity. Furthermore, concrete structure can be affected by incorporating SF in the concrete mixture. However, the total porosity could not be changed with the SF addition, but the large pores can be transformed into smaller pores and thereby altering the cement paste microstructure.

ACKNOWLEDGEMENT
This work was sponsored in part by "Scientific Research Fund Project of Xijing University (Grant No. XJ160135)"

References

1. A.P. Gursel, H. Maryman and C. Ostertag, *Journal of Cleaner Production*, 112 (2016) 823.
2. M. Aslam, P. Shafigh and M.Z. Jumaat, *Journal of Cleaner Production*, 126 (2016) 56.
3. H. Chen, S. Zhang, Z. Zhao, M. Liu and Q. Zhang, *Progress in Chemistry*, 31 (2019) 571.
4. W. Aperador, J. Duque and E. Delgado, *International Journal of Electrochemical Science*, 11 (2016) 3567.
5. K. Scrivener, F. Martirena, S. Bishnoi and S. Maity, *Cement and Concrete Research*, 114 (2018) 49.
6. D. Yuan, C. Zhang, S. Tang, X. Li, J. Tang, Y. Rao, Z. Wang and Q. Zhang, *Water research*, 163 (2019) 114861.
7. S. Tang, N. Li, D. Yuan, J. Tang, X. Li, C. Zhang and Y. Rao, *Chemosphere*, 234 (2019) 658.
8. P. Chindaprasirt and S. Rukzon, *Construction and building materials*, 22 (2008) 1601.
9. S.W.M. Supit and F.U.A. Shaikh, *Materials and structures*, 48 (2015) 2431.
10. P. Shao, J. Tian, F. Yang, X. Duan, S. Gao, W. Shi, X. Luo, F. Cui, S. Luo and S. Wang, *Advanced Functional Materials*, 28 (2018) 1705295.
11. C. Sun, S. Liu, J. Niu and W. Xu, *International Journal of Electrochemical Science*, 10 (2015) 5309.
12. E.I. Diaz-Loya, E.N. Allouche and S. Vaidya, *ACI materials journal*, 108 (2011) 300.
13. P. Shao, J. Tian, X. Duan, Y. Yang, W. Shi, X. Luo, F. Cui, S. Luo and S. Wang, *Chemical Engineering Journal*, 359 (2019) 79.
14. X. He, F. Deng, T. Shen, L. Yang, D. Chen, J. Luo, X. Luo, X. Min and F. Wang, *Journal of colloid and interface science*, 539 (2019) 223.
15. L. Yang, G. Yi, Y. Hou, H. Cheng, X. Luo, S.G. Pavlostathis, S. Luo and A. Wang, *Biosensors and Bioelectronics*, 141 (2019) 111444.
16. R. Bleszynski, R.D. Hooton, M.D. Thomas and C.A. Rogers, *Materials Journal*, 99 (2002) 499.
17. J. Hou and D. Chung, *Corrosion Science*, 42 (2000) 1489.

18. S. Fajardo, D.M. Bastidas, M. Ryan, M. Criado, D. McPhail, R. Morris and J. Bastidas, *Applied Surface Science*, 288 (2014) 423.
19. J. Arenas-Piedrahita, P. Montes-García, J. Mendoza-Rangel, H.L. Calvo, P. Valdez-Tamez and J. Martínez-Reyes, *Construction and building materials*, 105 (2016) 69.
20. N. Amudhavalli and J. Mathew, *International Journal of Engineering Sciences & Emerging Technologies*, 3 (2012) 28.
21. A. Col, V. Parry and C. Pascal, *Corrosion Science*, 114 (2017) 17.
22. A. Fahim, A.E. Dean, M.D. Thomas and E.G. Moffatt, *Materials and Corrosion*, 70 (2019) 328.
23. A. Bautista, G. Blanco and F. Velasco, *Cement and Concrete Research*, 36 (2006) 1922.
24. M. Gastaldi and L. Bertolini, *Cement and Concrete Research*, 56 (2014) 52.
25. P. Shao, L. Ding, J. Luo, Y. Luo, D. You, Q. Zhang and X. Luo, *ACS applied materials & interfaces*, 11 (2019) 29736.
26. R. Antunes, M. De Oliveira and I. Costa, *Materials and Corrosion*, 63 (2012) 586.
27. S. Kakooei, J. Rouhi, E. Mohammadpour, M. Alimanesh and A. Dehzangi, *Caspian Journal of Applied Sciences Research*, 1 (2012) 16.
28. C. Li, S. Hu, L. Yang, J. Fan, Z. Yao, Y. Zhang, G. Shao and J. Hu, *Chemistry–An Asian Journal*, 10 (2015) 2733.
29. Y. Chou, J. Yeh and H. Shih, *Corrosion Science*, 52 (2010) 2571.
30. W. Zhao, J. Zhao, S. Zhang and J. Yang, *International Journal of Electrochemical Science* 14 (2019) 8039.
31. A.T. Yousefi, S. Ikeda, M.R. Mahmood, J. Rouhi and H.T. Yousefi, *World Applied Sciences Journal*, 17 (2012) 524.
32. H. Luo, C. Dong, X. Li and K. Xiao, *Electrochimica Acta*, 64 (2012) 211.
33. P. Shao, X. Duan, J. Xu, J. Tian, W. Shi, S. Gao, M. Xu, F. Cui and S. Wang, *Journal of hazardous materials*, 322 (2017) 532.
34. S. Kakooei, H.M. Akil, A. Dolati and J. Rouhi, *Construction and Building Materials*, 35 (2012) 564.
35. J. Setina, A. Gabrene and I. Juhnevica, *Procedia Engineering*, 57 (2013) 1005.
36. F. Husairi, J. Rouhi, K. Eswar, C.R. Ooi, M. Rusop and S. Abdullah, *Sensors and Actuators A: Physical*, 236 (2015) 11.
37. R. Dalvand, S. Mahmud and J. Rouhi, *Materials Letters*, 160 (2015) 444.